

Chaotic Signature in Power Spectrum and Recurrence Quantification of Dynamical Behaviour of Multivariate Time Series

Abidemi Emmanuel Adeniji., Kayode Stephen Ojo and Adekunle Oluseye Sangotola

Received: 17 March 2024/Accepted: 01 May 2024 /Published: 08 May 2024

Abstract: This study investigates the presence of nonlinear dynamics and chaotic behaviour in air temperature, atmospheric pressure, and relative humidity using data collected from Lagos, Nigeria. Power spectral density analysis revealed an aperiodic nature with possible non-linear processes governing the time series. Recurrence quantification analysis (RQA) was employed to quantify the determinism and chaoticity within the data. Results suggest that all three variables (relative humidity, air temperature, and atmospheric pressure) exhibit evidence of both deterministic and chaotic behaviour. Deterministic behaviour was highest for air temperature, followed by pressure and then humidity. Conversely, chaoticity was highest for relative humidity, followed by pressure and then air temperature. These findings suggest complex underlying dynamics within the troposphere, potentially influenced by the region's convective nature and intense precipitation events. The observed determinism indicates some level of predictability, particularly for air temperature, while the chaoticity highlights the inherent complexity of atmospheric processes.

Keywords: Power Spectral Density, Underlying dynamics, Determinism, Low dimensional chaos.

Abidemi Emmanuel Adenij

Department of Physical Sciences, Bells University of Technology Ota, Ogun State.

Email: aeadeniji@bellsuniversity.edu.ng

Orcid id: 0000-0003-1930-5755

Kayode Stephen Ojo

Department of Physics, University of Lagos, Akoka, Yaba Lagos, Nigeria.

Email: kaojo@unilag.edu.ng

Orcid id: 0000-0002-3499-773X

Adekunle Oluseye Sangotola

Department of Physical Sciences, Bells University of Technology Ota, Ogun State, Nigeria

Email: aosangotola@bellsuniversity.edu.ng

Orcid id: 0009-0005-6621-8568

1.0 Introduction

Weather refers to the atmospheric state at a specific time and location. Factors such as atmospheric temperature, pressure, humidity, and wind are influential in shaping the weather conditions of a place (Amajama, *et al.*, 2023; Abimbola, *et al.*, 2021; Jacobson, 1999; Ukhurebor and Umukoro, 2018; Guidara, *et al.*, 2018). Most of the weather events take place in the troposphere which is the lower layer of the atmosphere near the Earth's surface (Ofure, *et al.*, 2017). The radio waves that pass through this layer are affected in both phase and amplitude by this nondispersive layer. Variations in these tropospheric meteorological parameters affect the properties of the atmosphere as a communication medium and are the main source of radio signal interference (Igwe, *et al.*, 2021; Eichie, *et al.*, 2017; Sabu, *et al.*, 2017; Isikwe, *et al.*, 2013; Joseph, 2016, 2016). Density, a crucial atmospheric property, fluctuates in response to weather variations (Okeke, *et al.*, 2019; Elechi and Otasowie, 2015; Helhel, *et al.*, 2008). Tropospheric density changes can affect how electromagnetic waves refract through different media with different densities, which

can affect the propagation properties (Amajama, *et al.*, 2023; Familusi, *et al.*, 2022; Agbo, *et al.*, 2013; Adediji and Ajewole, 2008; Willoughby, *et al.*, 2003). The degradation of radio signals in the troposphere can be categorized into two parts: background troposphere effects and turbulence. The slowly moving portion caused by the large-scale component, which corresponds to the input region, is primarily referred to as the background troposphere (Dong, 2019; Kolmogorov, 1968). The refractive index is a useful tool for characterizing radio wave propagation in the troposphere. When the refractive index is greater than 1, the propagation velocity slows down as the signal passes through the troposphere thereby introducing delay errors.

Generally, different delay errors can occur because of different atmospheric conditions. Because of the troposphere's heterogeneity, atmospheric variables like humidity, pressure, and temperature change depending on the height and spatial distribution of the refractive index, which bends the propagation path and introduces bending errors. Tropospheric turbulence encompasses the dynamic fluctuations resulting from small-scale vortices and aligns with the inertial subrange of turbulent motion. Under some severe weather situations, the meteorological factors fluctuate rapidly and intensely, causing random oscillations in the amplitude and phase of the signal (Dong, 2019). This tropospheric turbulence can be considered as a nonlinear process and chaotic behaviour that can be present in different regions of the atmosphere (Enugonda *et al.*, 2023). In the context of the atmosphere, some works have been carried out on radio refractivity using nonlinear dynamics and chaotic approaches (Ogunjo *et al.*, 2013; Adediji and Ogunjo, 2014; Fuwape and Ogunjo, 2016; Adelakun *et al.*, 2019; Ojo *et al.*, 2019; Adeniji, *et al.*, 2021; Fuwape, *et al.*, 2017). The Multifractal Detrended Fluctuation Analysis MF DFA method was applied to study

climate impacts and breakpoints in climate data and to understand how nonlinearity and multifractality occur in temperature data (Ogunjo, *et al.*, 2021; Lana, *et al.*, 2020; Silva, 2020; Agbazo, *et al.*, 2019; Garcia-Marin, *et al.*, 2019; Herrera-Grimaldi *et al.*, 2019; Krzyszczak *et al.*, 2019; Karatasou and Santamouris, 2018; Baranowski, *et al.*, 2015), relative humidity data (Bejoy, *et al.*, 2023) and wind data (Telesca and Lovallo, 2011).

Due to the non-availability of dynamical equations describing the underlying processes of the atmosphere, there is a need to investigate the nonlinearity and degree of chaoticity of atmospheric temperature, pressure, and humidity as they are responsible for the heterogeneity of the atmosphere.

1.1 Data and Pre-processing

Measurements of daily relative humidity, air temperature and atmospheric pressure were recorded at 5-min time intervals for a period of one year (1st January – December 2008) and collected from National Space Research and Development Agency (NASRDA). The data points used for the analysis range from 8064 to 8928 for the twelve months of the year. The study area is in the University of Lagos, Akoka weather station in the city of Lagos which lies in south-west Nigeria with a wet equatorial type of climate influenced by its nearness to the equator and the Gulf of Guinea. It is located at latitude $6^{\circ} 25'$ and $18.53''$ N and between longitude $3^{\circ} 19'$ and $21.50''$ E with an altitude of 3.3m. The interaction between the warm, humid maritime tropical air mass and the hot and dry continental air mass from the interior gives the state two seasons; a wet season from April to October and a dry season from November to March (Fasona *et al.*, 2005).

2.0 Materials and Methods

2.1 Power Spectral Density

According to Valsakumar, *et al.*, 1997, Let $x(t)$ be one of the state variables describing the



chaotic dynamical system. The time autocorrelation function of $x(t)$ is defined as

$$c(t) = \lim_{T \rightarrow \infty} \frac{1}{T} \int_0^{T-|t|} dt' x(t') x(t' + |t|). \tag{1}$$

The power spectrum $C(f)$ is defined as the Fourier transform of the autocorrelation function

$$C(f) = \int_{-\infty}^{\infty} c(t) e^{i2\pi ft} dt \tag{2}$$

Power spectrum can also be equivalently defined as the modulus square of its Fourier amplitude per unit time. This is given by

$$C(f) = \lim_{T \rightarrow \infty} \frac{1}{T} \left| \int_0^T x(t) e^{i2\pi ft} dt \right|^2$$

$$P(f, N, \tau) = \tau \sum_{j=-(N-1)}^{(N-1)} c_j(N) e^{j2\tau f \tau j} \tag{5}$$

It is also possible to express $P(f, N, \tau)$ like equation (3). Let $X(f, N, \tau)$ be the discrete Fourier transform of $\{x_j\}$,

$$X(f, N, \tau) = \sum_{j=0}^{N-1} x_j e^{j2\tau f \tau j} \tag{6}$$

and the corresponding power spectrum is

$$P(f, N, \tau) = \frac{\tau}{N} \langle |X(f, N, \tau)|^2 \rangle \tag{7}$$

$P(f, N, \tau)$ is referred to in this study as the computed power or just the power spectrum. In the following limit, the computed power spectrum $P(f, N, \tau)$ equals the true power spectrum $C(f)$.

$$C(f) = \lim_{\tau \rightarrow 0} \lim_{N \rightarrow \infty} P(f, N, \tau) \tag{8}$$

2.2 Determination of embedding dimension and time delay

Two crucial parameters that must be determined for the recurrence analysis from a time series are the embedding dimensions (m) and the delay time (τ), both of which are extensively discussed in the literature (Kantz and Schreiber 1997). The two common methods for estimating the ideal time delay (τ) are the mutual information approach and the autocorrelation method. In literature, the first approach is recommended for nonlinear time series analysis and is defined in Takens (1981).

$C(f)$ is defined in (2) and (3), therefore, is being taken to be the true power spectrum.

The next step is to define the power spectrum $P(f, N, \tau)$ of such a discrete scalar time series such that it agrees with $C(f)$ in the limit $\tau \rightarrow 0$ and $N \rightarrow \infty$. The discrete version of the autocorrelation is defined as

$$c_j(N) = \left\langle \frac{1}{N} \sum_{l=0}^{N-1-|j|} x_l x_{l+|j|} \right\rangle \tag{4}$$

The purpose of this averaging is to guarantee that, in the limit $N \rightarrow \infty$, the autocorrelation function of the continuous-time process $c(t)$ computed at $t = j\tau$ and the discrete-time series $c_j(N)$ are the same. $P(f, N, \tau)$ is then defined as

$$I(\tau) = - \sum_{i,j} p_{ij} \ln \frac{p_{ij}(\tau)}{p_i p_j}$$

where p_{ij} represents the joint probability of finding a time series value in the i^{th} interval and a time series value in the j^{th} interval following a time τ , and p_i represents the probability of finding a time series value in the i^{th} interval in the partition.

The following metrics are used to quantify the deterministic structure and complexity of RPs:



(i)Maxline (L_{max}) is the longest line segment measured parallel to the main diagonal in the plot.

$$DIV = \frac{1}{L_{max}}, \quad L_{max}(\{l_i; i = 1, \dots, N_l\})_{max} \quad (10)$$

According to Eckmann *et al.*, (1987), the highest positive Lyapunov exponent was inversely related to the longest diagonal line structure.

(ii)Determinism (DET) is the ratio of recurrence points forming diagonal structures (of at least length) to all recurrence points.

$$DET = \frac{\sum_{l=l_{min}}^N lP(l)}{\sum_{i,j} R_{i,j}} \quad (11)$$

where $P(l)$ is the frequency distribution of the diagonal line lengths (for a diagonal parallel to the main diagonal); l is the length of the line structure. Long diagonal lines depict periodic signals (e.g. sine waves), short diagonal lines depict chaotic signals and no diagonal lines depict stochastic signals (e.g., random numbers) Webber and Zbilut (2005).

3.0 Results and Discussion

3.1 Power spectral density analysis

We display in Fig. 1 (a-f) the Power spectral density diagrams for some selected months (January and December) for relative humidity, air temperature, and atmospheric pressure for both wet and dry seasons using equation (7). The power spectral density (PSD) diagrams of relative humidity, air temperature, and atmospheric pressure provide information on the character of fluctuations in the time series data. The (PSD) diagrams are derived based on the periodogram PSD estimation method which describes how the power of a time series is distributed with frequency. In all cases, there are no regular sharp peaks which is the representative of aperiodic nature of climate signals with the power increasing as the frequency goes down. There is the existence of periodic components in these time series which implies low predictability of these time series

and also, the existence of the higher harmonics in the spectra indicates that the processes underlying the time series are not linear, but there is some kind of nonlinearity (Bigdeli and Lafmejani, 2016; Timmer, *et al.*, 2000; Grassberger and Procaccia, 1983). It is observed that climate signals are found to exhibit an exponential decay followed by a much slower decay (like an algebraic decay) which are the hallmark of power spectra of chaotic dynamical systems (Marwan and Braun, 2023; Serykh and Sonechkin, 2019; Valsakumar *et. al*, 1997).

3.2 Choice of delay time and embedding dimension

Fig. 2 depicts the mutual information plotted against time delay for Relative humidity, air temperature and atmospheric Pressure. It is observed that the first minimum on the curve of mutual information versus time delay occurs at $\tau \geq 54$, $\tau \geq 66$ and $\tau \geq 65$ which are the suitable choices of time delay for relative humidity, air temperature and atmospheric pressure, respectively. Fig. 3 shows the plot of the percentage of the false nearest neighbour (FNN) versus the embedding dimension (m). The proper reconstruction of the state space from the available data is essential in modelling and prediction to successfully estimate the invariant properties of the embedded attractor (Matilla-García, *et al.*, 2021). The choice of the embedding dimension is essential in knowing the number of variables that can unfold the attractor in phase space and also, in extracting information about the system dynamics (Adeniji *et al.*, 2019). If we embed the time series once (i.e., into two dimensions) using some time delay, then we can use the coordinates of those data points to examine whether the distance between them has changed appreciably. The coordinates of those data points can be used to determine whether there has been a discernible change in the distance between them if we embed the time series once (i.e., into two dimensions) using a



time delay. False neighbours are identified when the distance between neighbours varies noticeably after embedding; this suggests that more embedding of the data is required. The attractor's shape remains unaltered after embedding, indicating that the current embedding size is enough, and they are referred to as true neighbours if their distance does not change significantly. This can be carried out for progressively increasing embedding

dimensions m , and we select a value for m at the point where either following embeddings remain unchanged or the number of FNN reduces to zero (Wallot and Mønster, 2018). The suitable choices of the false nearest neighbour depicted in Fig. 2 for relative humidity, air temperature and atmospheric pressure are dimensions $m \geq 10$, $m \geq 7$ and $m \geq 14$, respectively.

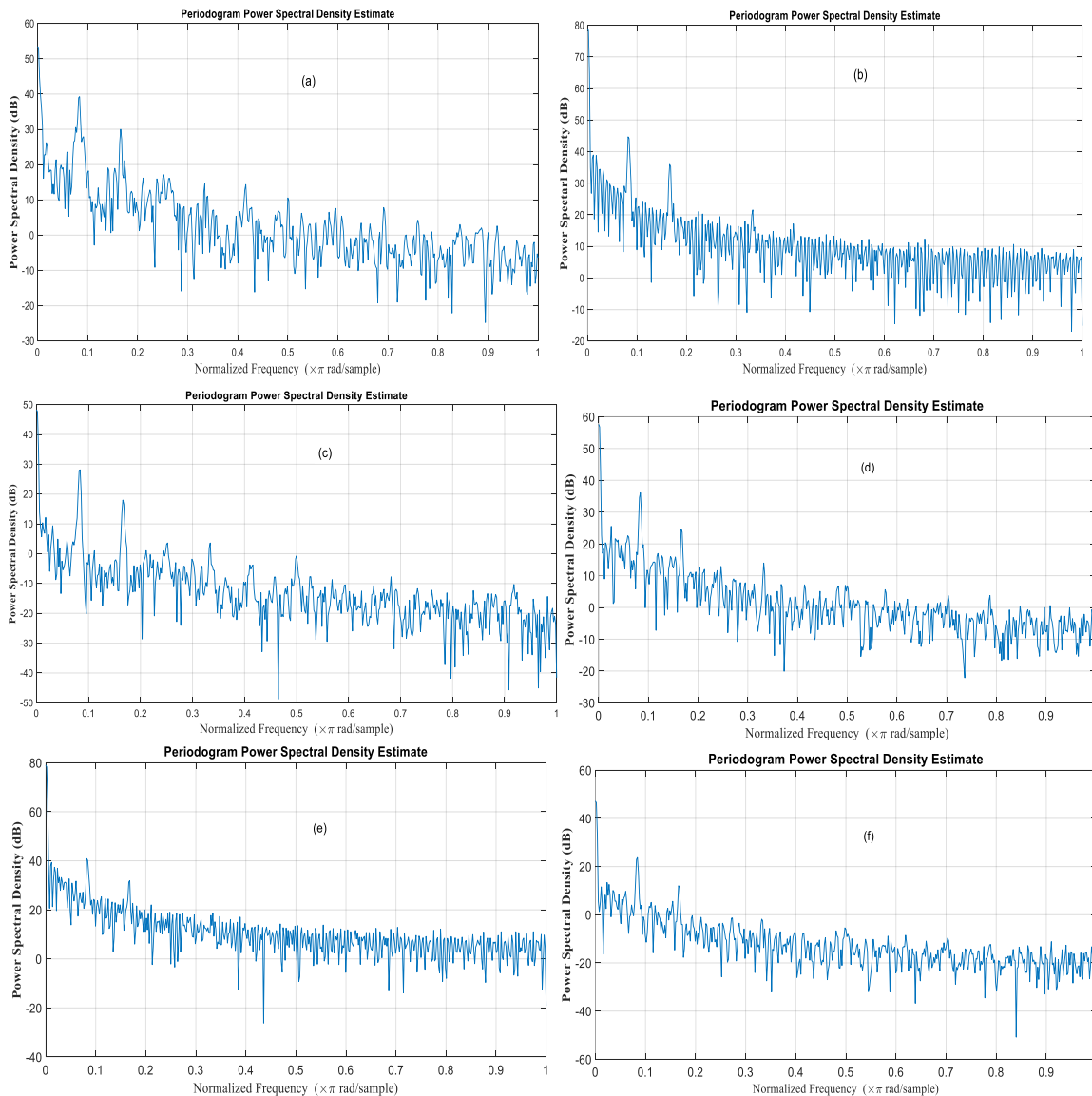


Fig. 1: Power spectral density in January for (a) relative humidity, (b) air temperature (c) atmospheric pressure, and December for (d) relative humidity (e)air temperature (f) atmospheric pressure.



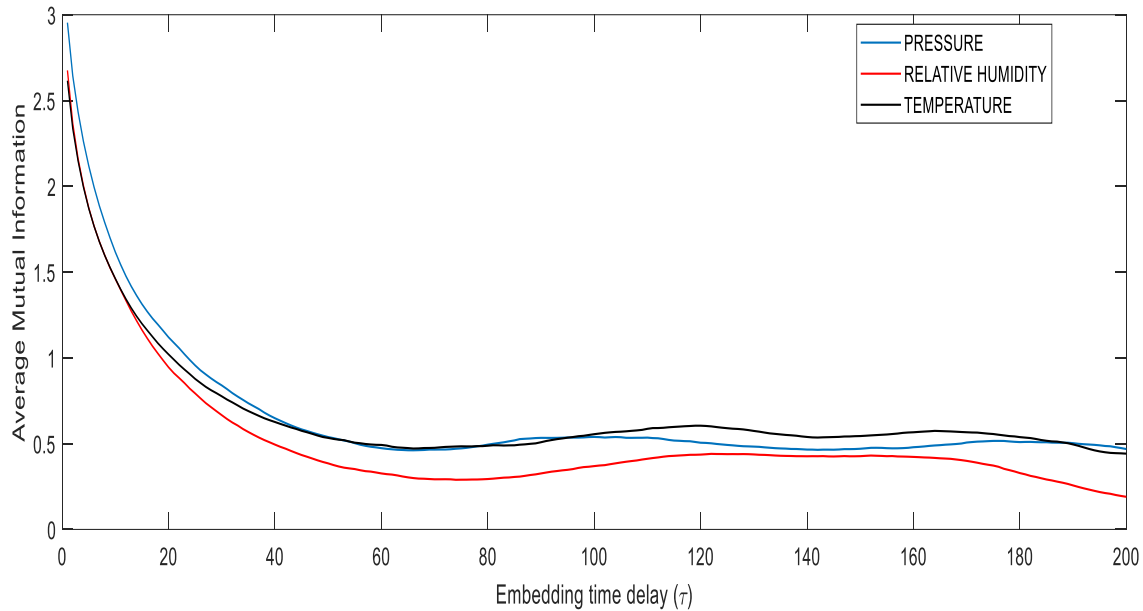


Fig. 2: Average mutual information versus Time delay (τ).

3.3 Recurrence Quantification Analysis (RQA)

Several methods have been proposed for choosing the radius of the attractor. A too-small value allows no recurrent patterns, too large values may result in false recurrences (Ding, *et al.*, 2008). Several rules of thumb have been proposed, such as a value corresponding to 1% of REC (Zbilut, *et al.*, 2002), $\varepsilon = 0.1\sigma$, where ε is the recurrence threshold, σ is the standard deviation of the time series, a value that does not exceed 10% of the mean or the maximum of the phase space (Ding, *et al.*, 2008; Schinkel, *et al.*, 2008). In this study, the method of 5-6% of the maximal space diameter of the attractor is chosen for the recurrence threshold suggested in Majid *et al.*, 2023. The recurrence threshold is chosen to be $0.05dA \leq \varepsilon \leq 0.06dA$ where ε is the recurrence threshold, and dA is the maximum attractor diameter. Euclidean norm is used for the recurrence quantifiers.

RQA values are displayed in Table 1, which shows the values of the divergence for the twelve months ranging from 0.0909 to 0.5000 for relative humidity, 0.003802 to 0.017289 for

air temperature and 0.05 to 0.333333 for atmospheric pressure. Determinism (predictability) values range from 0.0372671 to 0.322709 for relative humidity, 0.942476 to 0.972998 for air temperature, and 0.132972 to 0.658588 for atmospheric pressure, respectively.

From the bar chart in Fig. 4, we observed that there is evidence of deterministic chaos and fluctuation in the dynamical behaviour of relative humidity, air temperature and atmospheric pressure. The highest chaoticity is exhibited in relative humidity, followed by atmospheric pressure while air temperature exhibited the lowest throughout the year. The high chaoticity exhibited in relative humidity is attributed to the high concentration of water vapor which also increases the complexity of the troposphere. The variations in chaoticity are linked to the dynamical transitions caused by different changes in climate and characteristics of intermittence in the troposphere. It could also be attributed to the fact that West Africa is convective, especially with precipitation and intense rain rates provided by the mesoscale convective system according to Kof *et al.*, 2014.



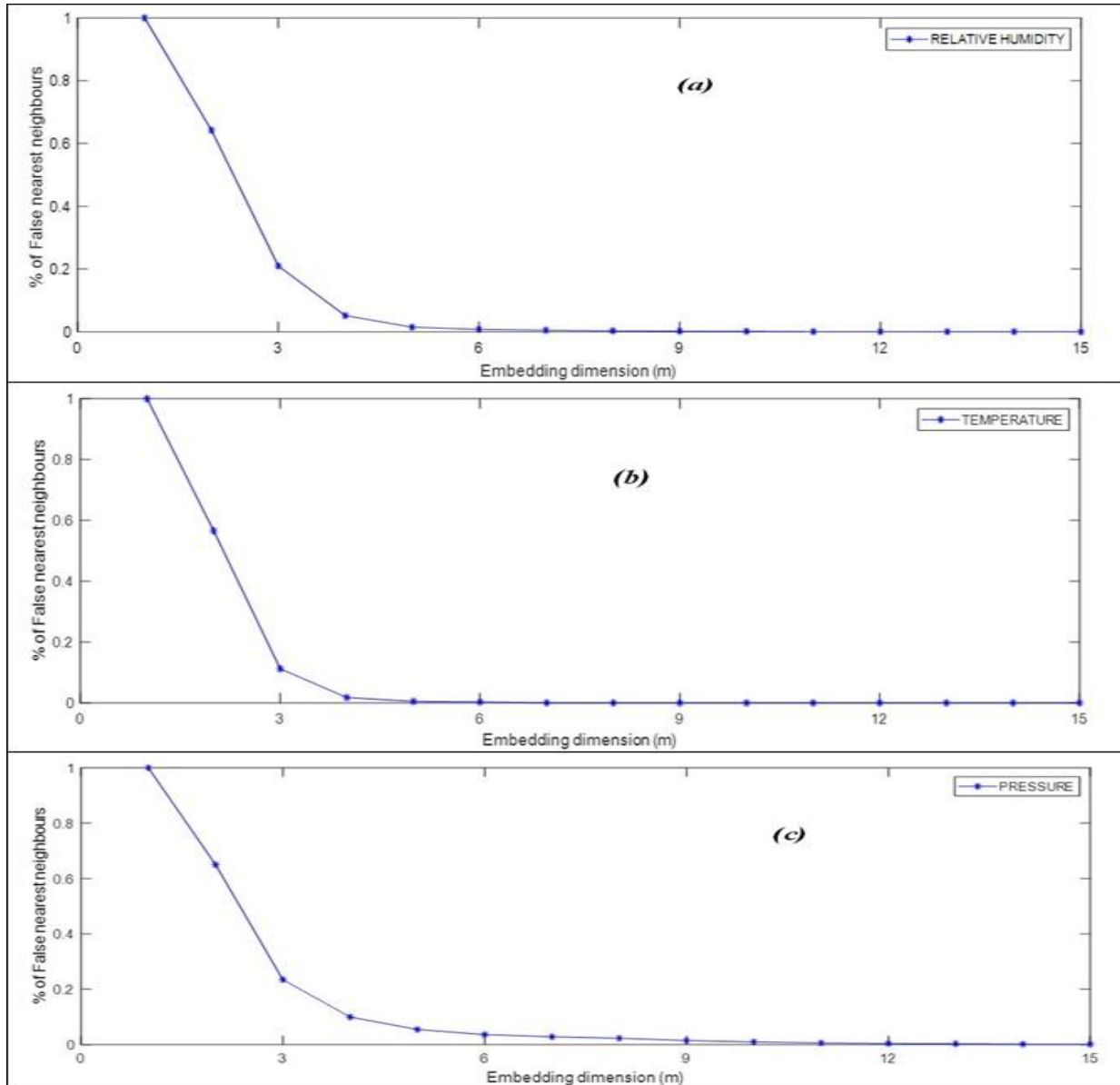


Fig. 3: Percentage of false nearest neighbour versus embedding dimension (m) for (a) relative humidity (b) atmospheric pressure (c) air temperature.

From the bar chart in Fig. 5, there is evidence of determinism (DET) in the dynamical behaviour of relative humidity, air temperature and atmospheric pressure throughout the year. The highest determinism (predictability) is observed in air temperature, followed by atmospheric pressure while the lowest is observed in relative humidity. The highest determinism observed in air temperature

implies a high length of prediction of the future evolution of the dynamics underlying air temperature, followed by atmospheric pressure while the lowest is observed in relative humidity. From the quantification analysis using RQA the underlying dynamics of relative humidity, air temperature and atmospheric pressure are classified as either quasi-periodic or low-dimensional chaotic.



Table 1: Recurrence quantifiers for relative humidity, air temperature, and atmospheric pressure.

Month	Relative Humidity		Air temperature		Atmospheric pressure	
	DIV	DET	DIV	DET	DIV	DET
Jan	0.333333	0.147436	0.004557	0.970917	0.142857	0.28953
Feb	0.25	0.179431	0.009744	0.962231	0.25	0.132972
Mar	0.5	0.0372671	0.007242	0.942476	0.166667	0.262402
Apr	0.333333	0.194805	0.005545	0.960653	0.083333	0.486576
May	0.5	0.081081	0.003802	0.968707	0.076923	0.487591
Jun	0.090909	0.268501	0.005449	0.967549	0.142857	0.512392
Jul	0.090909	0.322709	0.010481	0.972924	0.05	0.658588
Aug	0.25	0.13289	0.012594	0.947748	0.1	0.390265
Sep	0.083333	0.317378	0.008592	0.95958	0.066667	0.542105
Oct	0.333333	0.096491	0.005603	0.947208	0.25	0.270627
Nov	0.166667	0.169912	0.017289	0.967398	0.333333	0.209627
Dec	0.2	0.236464	0.012123	0.972998	0.2	0.358283

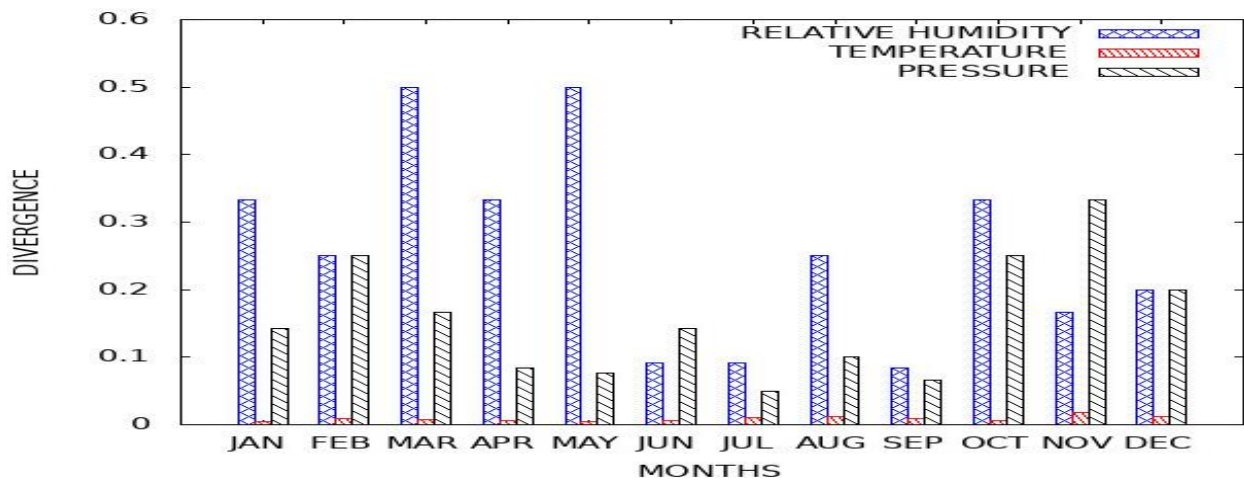


Fig. 4: Divergence (Chaoticity) for the relative humidity, air temperature and atmospheric pressure

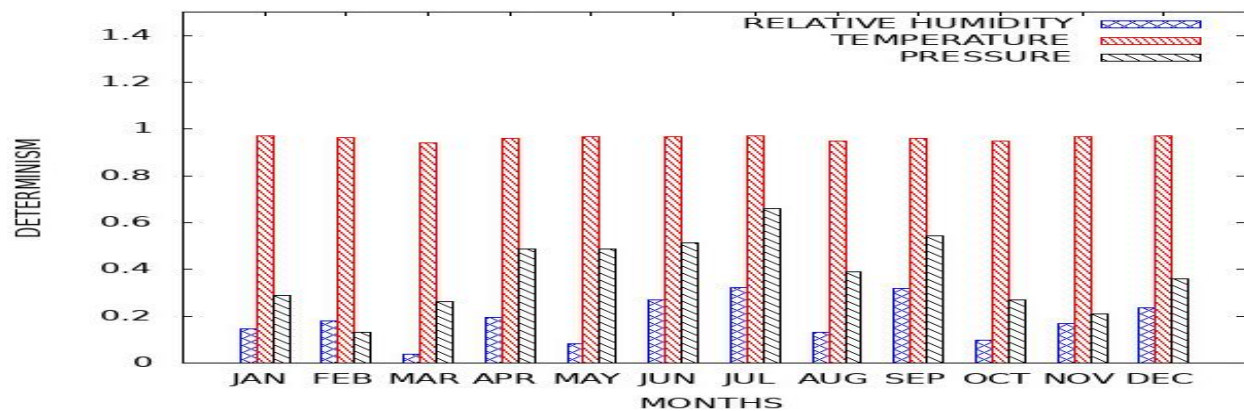


Fig. 5: Determinism (DET) for the relative humidity, air temperature and atmospheric pressure



4.0 Conclusion

The analysis of atmospheric temperature, pressure, and humidity data from Lagos, Nigeria revealed evidence of both deterministic and chaotic behaviour within these variables. Deterministic behaviour was most prominent in air temperature, indicating a greater degree of predictability compared to relative humidity and atmospheric pressure. Conversely, relative humidity exhibited the highest level of chaoticity, signifying a more complex and unpredictable system. These findings point towards intricate underlying dynamics governing the troposphere in this region, likely influenced by factors such as its convective nature and frequent heavy precipitation events. This study provides a valuable starting point for further exploring the nonlinear dynamics of the troposphere. Future research efforts could benefit from:

- Expanding the analysis to incorporate additional atmospheric variables for a more comprehensive understanding of tropospheric interactions.
- Investigating the influence of seasonal variations on the observed dynamics using data spanning multiple years.
- Employing more advanced techniques, such as machine learning algorithms, to enhance the prediction capabilities for atmospheric processes. By incorporating these recommendations, future studies can delve deeper into the complexities of the troposphere and contribute to improved weather forecasting models.

5.0 Acknowledgement

The analysis of the results presented in this paper relies on Tropospheric Data Acquisition Network (TRODAN) data which is managed by the Centre for Atmospheric Research, National Space Research and Development Agency, Federal Ministry of Science and Technology, Anyigba, Nigeria. We would like to express our profound gratitude to the Centre

for Atmospheric Research and their partners for promoting high standards of atmospheric observatory practice as well as the Federal Government of Nigeria for continuous funding of the Nigerian Space programme (www.carnasrda.com).

6.0 References

- Adediji, A. T., & Ajewole, M. O. (2008). Vertical profile of radio refractivity gradient in Akure, South-West, Nigeria. *Progress in Electromagnetics Research C*, 4, 157–168.
- Adediji, A. T., & Ogunjo, S. T. (2014). Variations in non-linearity in vertical distribution of microwave radio refractivity. *Progress in Electromagnetics Research M*, 36, 177–183.
- Adelakun, A. O., Ojo, J. S., & Edward, O. V. (2020). Quantitative analyses of complexity and nonlinear trend of radio refractivity gradient in the troposphere. *Advances in Space Research*, 65(9), 2203–2215.
- Adeniji, A. E., Olusola, O. I., & Njah, A. N. (2018). Comparative study of chaotic features in hourly wind speed using recurrence quantification analysis. *AIP Advances*, 8, 025102. <https://doi.org/10.1063/1.4998674>
- Adeniji, A. E., Ajeigbe, E. M., & Ojo, K. S. (2021). Characterization and investigation of nonlinear behaviour of radio refractivity during the rainy and dry seasons in the coastal region of Nigeria. *Journal of Applied Sciences & Environmental Management*, 25(7), 1125–1131.
- Abimbola, O. J., Bada, S. O., Falaiye, A. O., Sukam, Y. M., Otto, M. S., & Muhammad, S. (2021). Estimation of radio refractivity from satellite-derived meteorological data over a decade for West Africa. *Scientific African*, 14, 1054.



- Agbazo, M., Koto Nogobi, G., Alamou, E., Kounouhewa, B., Afouda, A., & Kounkonnou. (2019). Multifractal behaviors of daily temperature time series observed over Benin synoptic stations (West Africa). *Earth Science Research Journal*, 23, 365–373.
- Agbo, A. G., Okoro, N. O., & Amechi, O. A. (2003). Atmospheric refractivity over Abuja, Nigeria. *International Research Journal of Pure and Applied Physics*, 1(1), 37–45.
- Amajama, J., Asagha, E. N., Ushie, O. J., Iwuji, P. C., Akwagiobe, J. U., Faithpraise, F. O., Ikeuba, A. I., & Basse, D. E. (2023). Radio refractivity impact on signal strength of mobile communication. *Journal of Electrical and Computer Engineering*, 2023, Article ID 3052241. <https://doi.org/10.1155/2023/3052241>
- Baranowski, P., Krzyszczyk, J., Slawinski, C., Hoffmann, H., Kozyra, J., Nierobca, A., Siwek, K., & Gluza, A. (2015). Multifractal analysis of meteorological time series to assess climate impacts. *Climate Research*, 65, 39–52.
- Bejoy, J. J., Dave, J., & Ambika, G. (2023). Multifractal and recurrence measures from meteorological data of climate zones in India. *arXiv:2307.01165v2 [physics.ao-ph]*.
- Bigdeli, N., & Lafmejani Sadegh, H. (2016). Dynamic characterization and predictability analysis of wind speed and wind power time series in Spain wind farm. *Journal of AI and Data Mining*, 4(1), 103–116.
- da Silva, H. S., Silva, J. R. S., & Stosi, T. (2020). Multifractal analysis of air temperature in Brazil. *Physica A: Statistical Mechanics and its Applications*, 549, 124333.
- Ding, H., Crozier, S., & Wilson, S. (2008). Optimization of Euclidean distance threshold in the application of recurrence quantification analysis to heart rate variability studies. *Chaos, Solitons & Fractals*, 38(5), 1457–1467. <https://doi.org/10.1016/j.chaos.2008.02.013>
- Dong, X., Hu, J., Hu, C., Long, T., Li, Y., & Tian, Y. (2019). Modeling and quantitative analysis of tropospheric impact on inclined geosynchronous SAR imaging. *Remote Sensing*, 11(8), 803. <https://doi.org/10.3390/rs11070803>
- Eckmann, J. P., Kamphorst, S., & Ruelle, D. (1987). Recurrence plots of dynamical systems. *Europhysics Letters*, 4, 973–977.
- Eichie, J. O., Oyedum, O. D., Ajewole, M. O., & Aibinu, A. M. (2017). Artificial Neural Network model for the determination of GSM Rxlevel from atmospheric parameters. *Engineering Science and Technology, an International Journal*, 20(2), 795–804.
- Elechi, P., & Otasowie, P. (2015). Determination of GSM signal penetration loss in some selected buildings in Rivers State, Nigeria. *Nigerian Journal of Technology*, 34(3), 609–615.
- Enugonda, R., Anandan, V. K., & Ghosh, B. (2023). A new approach to atmospheric turbulence measurements using HOSE on radar backscattered echoes. *Journal of Atmospheric and Solar-Terrestrial Physics*, 243, 106023.
- Familusi, T. O., Ewetumo, T., Adedayo, K. D., & Ojo, J. S. (2022). Assessment of radio refractivity and frequency modulated radio signal strength variability with time in broadcasting system using Osun State Broadcasting Cooperation (OSBC), FM 104.5 MHz as a reference station. *International Journal of Innovative Science and Research Technology*, 7(4), 1479–1489.
- Fasona, M., Omojola, A., Odunuga, S., Tejuoso, O., & Amogu, N. (2005). An appraisal of sustainable water management solutions for large cities in



- developing countries through GIS: The case of Lagos, Nigeria. In Proceedings of the Symposium S2 Held during the 7th IAHS Scientific Assembly, Foz do Iguacu, Brazil, 3–9, 49–57.
- Fraser, A. M., & Swinney, H. I. (1986). Independent coordinates for strange attractors from mutual information. *Physical Review A*, 33, 1134–1140.
- Fuwape, I. A., Ogunjo, S. T., Oluyamo, S. S., & Rabi, A. B. (2017). Spatial variation of deterministic chaos in mean daily temperature and rainfall over Nigeria. *Theoretical and Applied Climatology*, 130, 119–132. <https://doi.org/10.1007/s00704-016-1867-x>
- Fuwape, I. A., & Ogunjo, S. T. (2016). Quantification of scaling exponents and dynamical complexity of microwave refractivity in a tropical climate. *Journal of Atmospheric and Solar-Terrestrial Physics*, 150–151, 61–68.
- Garcia-Marin, P., Estevez, J., Alcalan-Miras, J. A., Morbidelli, R., Flammini, A., & Ayuso-Munoz, J. L. (2019). Multifractal analysis to study break points in temperature data sets. *Chaos: An Interdisciplinary Journal of Nonlinear Science*, 29, 093116.
- Grassberger, P., & Procaccia, I. (1983). Measuring the strangeness of strange attractors. *Physica D: Nonlinear Phenomena*, 9, 189–208.
- Guidara, A., Fersi, G., Derbel, F., & Jemaa, M. B. (2018). Impacts of temperature and humidity variations on RSSI in indoor wireless sensor networks. *Procedia Computer Science*, 126, 1072–1081.
- Helhel, S., Ozen, S., & Goksu, H. (2008). Investigation of GSM signal variation against dry and wet earth effects. *Progress in Electromagnetics Research B*, 1, 147–157.
- Herrera-Grimaldi, P., Garcia-Marin, A. P., & Estevez, J. (2019). Multifractal analysis of diurnal temperature range over southern Spain using validated datasets. *Chaos*, 29, 063105.
- Igwe, K., Oyedum, O., Aibinu, A., Ajewole, M., & Moses, A. (2021). Application of artificial neural network modeling techniques to signal strength computation. *Heliyon*, 7(3), e06047–e06049.
- Isikwe, C. B., Kwen, A. Y., & Chamegh, M. T. (2013). Variations in the tropospheric surface refractivity over Makurdi, Nigeria. *Research Journal of Earth and Planetary Sciences*, 3(2), 50–59.
- Jacobson, M. Z. (1999). *Fundamentals of Atmospheric Modeling*. Cambridge University Press.
- Joseph, A. (2016). Impact of temperature on UHF radio signal. *International Journal of Engineering Research and General Science*, 4(2), 619–622.
- Joseph, A. (2016). Force of atmospheric humidity on (UHF) radio signal. *International Journal of Scientific Research Engineering and Technology*, 5(2), 56–59.
- Kantz, H., & Schreiber, T. (1997). *Nonlinear Time Series Analysis*. University Press, Cambridge.
- Karatasou, S., & Santamouris, M. (2018). Multifractal analysis of high-frequency temperature time series in the urban environment. *Climate*, 6, 50.
- Kof, A. K., Gosset, M., Zahiri, E., Ochou, A. D., Kacou, M., Cazenave, F., & Assamoi, P. (2014). Evaluation of X-band polarimetric radar estimation of rainfall and rain drop size distribution parameters in West Africa. *Atmospheric Research*, 143, 438–461. DOI:10.1016/j.atmosres.2014.03.009
- Kolmogorov, A. N. (1968). Local structure of turbulence in an incompressible viscous fluid at very high Reynolds numbers. *Physics-Uspekhi*, 10, 734–746.



- Krzyszczak, J., Baranowski, P., Zubik, M., Kazandjiev, V., Georgieva, V., Slawinski, C., Siwek, K., Kozyra, J., & Nierobca, A. (2019). Multifractal characterization and comparison of meteorological time series from two climatic zones. *Theoretical and Applied Climatology*, 137, 1811–1824.
- Lana, X., Rodriguez-Sola, R., Martinez, M. D., Casas-Castillo, M. C., Serra, C., & Kirchner, R. (2020). Multifractal structure of the monthly rainfall regime in Catalonia (NE Spain): Evaluation of the non-linear structural complexity. *Chaos*, 30, 073117.
- Majid, M. A., Noorani, M. S.M., & Razak, F.A. (2023). Nonlinear Dynamic Analysis of Meteorological Variables for Ha'il Region, Saudi Arabia, for the Period 1990-2022. *FME Transactions*, 51, 231-242.
- Marwan, N., & Braun, T. (2023). Power spectral estimate for discrete data. *Chaos*, 33(5), 053118. <https://doi.org/10.1063/5.0143224>.
- Matilla-García, M., Morales, I., Rodríguez, J.M., & Marín, M.R. (2021). Selection of Embedding Dimension and Delay Time in Phase Space Reconstruction via Symbolic Dynamics. *Entropy*, 23(2), 221. <https://doi.org/10.3390/e23020221>.
- Ofure, E. J., David, O. O., Oludare, A. M., & Musa, A. A. (2017). Impact of some atmospheric parameters on GSM signals, 13th Int. Conf. Electron. Comput. Comput. ICECCO 2017.
- Ogunjo, S. T., Ojo, J. S., Adediji, A. T., Adedayo, K. A., & Dada, J. B. (2013). Chaos in radio refractivity over Akure, South-Western Nigeria. In 5th Annual Conference of the Nigeria Union of Radio Science (NURS), 56-63.
- Ogunjo, S. T., Fuwape, I., & Rabi, A. B. (2021). Multifractal analysis of air and soil temperatures. *Chaos*, 31, 033110.
- Ojo, J. S., Adelakun, A. O., & Edward, O. V. (2019). Comparative study on Radio Refractivity Gradient in the troposphere using Chaotic Quantifiers. *Heliyon*, 5, e02083.
- Okeke, N. B., Isaac-Onerime, O. S., Okoge, O. V., & Nuhu, A. T. (2019). Study of the radio refractivity over Akwa, South Eastern Nigeria using meteorological parameters on the troposphere during dry and wet seasons. *IOSR Journal of Physics*, 11, 2, pp. 62–67.
- Sabu, S., Renimal, S., Abraham, D., & Premlet, B. (2017). A study on the effect of temperature on cellular signal strength quality. In *Proceedings of the International Conference on Nextgen Electronic Technologies*, pp. 38–41, Chennai, India.
- Schinkel, S., Dimigen, O., & Marwan, N. (2008). Selection of recurrence threshold for signal detection. *The European Physical Journal Special Topics*, 164, 1, pp. 45–53. <https://doi.org/10.1140/epjst/e2008-00833-5>.
- Serykh, I. V., & Sonechkin, D. M. (2019). Nonchaotic and globally synchronized short-term climatic variations and their origin. *Theoretical and Applied Climatology*, 137, 3-4, pp. 2639–2656. <https://doi.org/10.1007/s00704-018-02761-0>.
- Takens, F. (1981). Dynamical systems and turbulence. *Lecture notes in mathematics, Springer, London*, 898, pp. , 366–381. Detecting strange attractors in turbulence.
- Telesca, L., & Lovallo, M. (2011). Analysis of the time dynamics in wind records by means of multifractal detrended fluctuation analysis and the fisher - Shannon information plane. *Journal of Statistical Mechanics: Theory and Experiment*, P07001.
- Timmer, J., Haussler, S., Lauk, M., & Lucking, C. H. (2000). Pathological tremors:



deterministic chaos or nonlinear stochastic oscillators? *Chaos*, 10, 1, pp. 278-288.

Ukhurebor, K., & Umukoro, O. (2018). Influence of meteorological variables on UHF radio signal: recent findings for EBS, Benin City, South-South, Nigeria. IOP Conference Series: *Earth and Environmental Science*, 173, pp. 012017-012018.

Valsakumar, M.C., Satyanarayana, S.V.M., & Sridhar, V. (1997). Signature of chaos in power spectrum. *PRAMANA- Journal of Physics*, 48, 1, pp. 69-85.

Wallot, S., & Mønster, D. (2018). Calculation of average mutual information (AMI) and false-nearest neighbors (FNN) for the estimation of embedding parameters of multidimensional time series in MATLAB. *Frontiers in Psychology*, 9, 1679.

<https://doi.org/10.3389/fpsyg.2018.01679>

Webber, C. L., & Zbilut, J. P. (2005). *Recurrence quantification analysis. recurrence quantification analysis of nonlinear dynamical systems*, pp. 27–94. <http://www.nsf.gov/sbe/bcs/pac/nmbs/nmbs.jsp>.

Willoughby, A. A., Adimula, I. A., & Sorunke, A. O. (2003). Characteristics of surface radio refractivity over Ilorin, Nigeria.

Nigerian Journal of Physics, 15, 1, pp. 45-46.

Zbilut, J. P., Zaldívar-Comenges, J.-M., & Strozzi, F. (2002). Recurrence quantification based Lyapunov exponents for monitoring divergence in experimental data. *Physics Letters A*, 297, 3, pp. 173–181.

Compliance with Ethical Standards

Declarations:

The authors declare that they have no conflict of interest.

Data availability

All data used in this study will be readily available to the public.

Consent for publication

Not Applicable.

Availability of data and materials:

The publisher has the right to make the data public.

Competing interests

The authors declared no conflict of interest.

Funding

The authors declared no source of funding.

Authors' Contributions

Conceptualization of the work was done by Adeniji, A. E., while all authors were involved in the development of the manuscript and review.

